Entanglement properties of the nontrivial Haldane insulator in the 1D extended Bose-Hubbard model

2015 J. Phys.: Conf. Ser. 592 012134

(http://iopscience.iop.org/1742-6596/592/1/012134)

Journal of Physics: Conference Series **592** (2015) 012134 doi:10.1088/1742-6596/592/1/012134

Entanglement properties of the nontrivial Haldane insulator in the 1D extended Bose-Hubbard model

Satoshi Ejima and Holger Fehske

Institut für Physik, Ernst-Moritz-Arndt-Universität Greifswald, 17489 Greifswald, Germany

E-mail: <ejima,fehske>@physik.uni-greifswald.de

Abstract. We investigate the entanglement properties of a nontrivial topological phase in the one-dimensional (1D) Bose-Hubbard model with additional nearest-neighbor repulsion. Employing the large-scale density-matrix renormalization group technique we show that a gapped insulating phase protected by lattice inversion symmetry, the so-called Haldane insulator, appears between the Mott and density wave phases in the intermediate-coupling regime. The phase boundaries were determined from the central charge via the von Neumann entropy. The Haldane insulator reveals a characteristic degeneracy in the entanglement spectra. Breaking the lattice inversion symmetry strongly affects the distinctive gapped dispersion of the dynamical charge response of the bosonic Haldane insulator.

1. Introduction

In the recent past, quantum spin chains, featuring rich physics in spite of their simplicity, have attracted renewed attention from a topological point of view. For example, a novel symmetry-protected topological (SPT) phase, the gapful Haldane phase [1] protected by lattice inversion symmetry, appears in one-dimensional (1D) integer-spin systems [2, 3]. Interestingly such SPT phase emerges also in interacting boson systems with long-range particle replusion [4, 5, 6]. This is documented for the 1D extended Bose-Hubbard model (EBHM) with local and nearest-neighbor particle repulsion, and a site occupation $n_j = 0$, 1 or 2, where the system can be mapped into an effective spin-1 model with $S_j^z = n_j - \rho$ for a mean boson filling factor $\rho = 1$. Here the so-called Haldane insulator (HI) phase, resembling the topological Haldane phase in the quantum spin-1 chain, appears between the conventional Mott insulator (MI) and the insulating density wave (DW) phases in the intermediate-coupling regime. Thereby the MI-HI transition belongs to the Tomonaga-Luttinger liquid university class with central charge $c = 1$, while the HI-DW transition is of Ising type with $c = 1/2$ [5].

In this work we characterize the properties of the topological HI phase in the EBHM from an entanglement point of view. Utilizing the density-matrix renormalization group (DMRG) technique [7], we numerically determine the MI-HI and HI-DW quantum phase transition points via the central charge. The results appear to be in accordance with field theoretical predictions. For the nontrivial HI phase a distinctive degeneracy of the lowest entanglement levels is demonstrated. Finally, carrying out the dynamical DMRG (DDMRG) simulations [8, 9], we investigate the dynamical density structure factor in the vicinity of the quantum phase transitions to confirm the closing of the excitation gap, which is of great significance for the the SPT state.

2. Model and Method

The Hamiltonian of the EBHM reads

$$\hat{\mathcal{H}} = -t\sum_j(\hat{b}_j^\dagger\hat{b}_{j+1} + \hat{b}_j\hat{b}_{j+1}^\dagger) + U\sum_j \hat{n}_j(\hat{n}_j - 1)/2 + V\sum_j \hat{n}_j\hat{n}_{j+1}, \tag{1}$$

where $\hat{b}_j^\dagger$, $\hat{b}_j$, and $\hat{n}_j = \hat{b}_j^\dagger\hat{b}_j$ are, respectively, the boson creation, annihilation, and number operators at lattice site j. In Eq. (1) the nearest-neighbor boson transfer amplitude is denoted by t; U (V) parametrizes the on-site (nearest-neighbor) repulsions of bosons. The bosonic hopping amplitude t promotes a superfluid (SF) phase at weak interactions, while U (V) tends to stabilize a MI (DW) state. In what follows we take t as energy unit.

To address the topological properties of the 1D EBHM we perform an entanglement analysis in the framework of the finite-system DMRG approach. Considering the reduced density matrix $\rho_\ell = \mathrm{Tr}_{L-\ell}[\rho]$ of a sub-block of length ℓ, the entanglement spectrum ξ_α [10] is obtained from the weights λ_α of ρ_ℓ by $\xi_\alpha = -2\ln\lambda_\alpha$. In the nontrivial HI phase of the EBHM one expects a characteristic degeneracy of the lowest entanglement levels due to the artificial edges that appear by dividing the system into two sub-blocks during the simulation [11].

The entanglement analysis provides also valuable information about the universality class of the system. Adding up the λ_α in the course of their computation, the von Neumann entropy is obtained as $S_L(\ell) = -\mathrm{Tr}_\ell[\rho_\ell\ln\rho_\ell]$. Exploiting the conformal field theory result $S_L(\ell) = \frac{c}{3}\ln\left[\frac{L}{\pi}\sin\left(\frac{\pi\ell}{L}\right)\right] + s_1$ (s_1 is a non-universal constant), the central charge c can be computed from the relation [12]

$$c^*(L) = \frac{3[S_L(L/2-1) - S_L(L/2)]}{\ln[\cos(\pi/L)]}\,, \tag{2}$$

and the phase boundaries follow—in a very efficient and accurate manner— from the numerically determined c^*, because the system becomes critical only at the MI-HI (HI-DW) transition points where $c = 1$ ($c = 1/2$) and c^* forms pronounced peaks as the system size increases. Quite recently this has been demonstrated for the EBHM [6].

In order to characterize the various insulating phases the excitation gaps have to be examined, which behave differently approaching the trivial-nontrivial phase transition points, where one expects the gap closing. This was also shown for the EBHM [4, 5, 6]. While the single-particle gap $\Delta_c = E_0(N+1) + E_0(N-1) - 2E_0(N)$ is finite in the MI, HI and DW phases and closes at the MI-HI transition, the neutral gap $\Delta_n = E_1(N) - E_0(N)$ closes at both the MI-HI and HI-DW transition lines. Here, $E_0(N)$ and $E_1(N)$ are the energies of the ground state and first excited state of the N-particle system, respectively, which can be easily calculated by DMRG.

Finally, calculating the dynamical charge structure factor is of particular importance since the frequency- and wave-vector-resolved density response can be directly compared with experimental results by momentum-resolved Bragg spectroscopy [13, 14]. The charge structure factor is defined as

$$S(k,\omega) = \sum_n |\langle\psi_n|\hat{n}_k|\psi_0\rangle|^2\delta(\omega - \omega_n)\,, \tag{3}$$

where $|\psi_0\rangle$ ($|\psi_n\rangle$) denotes the ground state (nth excited state) and $\omega_n = E_n - E_0$ is the corresponding excitation energy. In the absence of the nearest-neighbor repulsion V, $S(k,\omega)$ was intensively studied by means of perturbation theory and the DDMRG method [15, 16]. Taking V into account, it is shown that the dispersion of $S(k,\omega)$ in the HI phase is remindful of those of the spin-1 Heisenberg chain and behaves very differently in all three insulating phases [6]. Hence $S(k,\omega)$ might be used analyzing experiments in order to discriminate the various insulator

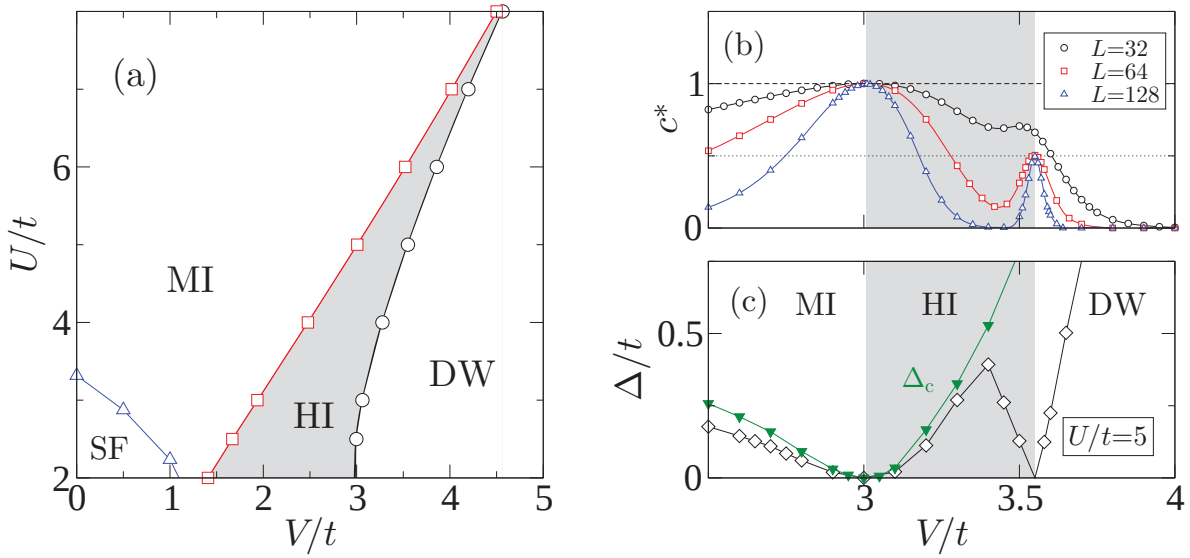

Figure 1. Ground-state phase diagram of the constrained extended Bose-Hubbard model with $n_b = 3$ and $\rho = 1$, showing the Mott insulator (MI), Haldane insulator (HI), density wave (DW) and superfluid (SF) phases. The MI-HI (squares) [HI-DW (circles)] phase transitions are determined by the central charge $c = 1$ [$c = 1/2$] exploiting the von Neumann entropy as demonstrated in panel (b) for $U/t = 5$. Panel (c) gives the corresponding ($L \to \infty$ extrapolated) data of the single-particle gap (triangles) and neutral gap (diamonds). The shaded regions in panels (b) and (c) define the HI phase.

states. Here we adapt the DDMRG method to simulate $S(k, \omega)$ in the HI phase of the EBHM, especially near MI-HI and HI-DW transition points with a focus on the gap closing.

In this work we fix the maximum number of bosons per site $n_b = 3$. Furthermore, we use periodic boundary conditions (PBC) and keep up to $m = 2400$ density matrix states in the DMRG computation, so that the discarded weight is typically smaller than 1×10^{-7}. For the DDMRG simulations we take $m = 800$ states to compute the ground state during the first five sweeps, and afterwards use 400 states evaluating dynamical quantities.

3. Numerical results

Figure 1(a) displays the DMRG ground-state phase diagram of the 1D EBHM (1) with $n_b = 3$. It exhibits three different insulating phases, besides a superfluid state in the weak-coupling region. We have shown in a preceding work that the phase boundaries between these insulating phases can be determined from the numerically calculated central charge c^* [6]. This works particularly well in the intermediate-coupling regime as demonstrated by Fig. 1(b). Obviously two maxima develop in c^*, which become more and more pronounced as the system size L increases, indicating the MI-HI and HI-DW transitions with $c = 1$ and $1/2$, respectively. This shows that the system becomes critical approaching the quantum phase transition points. Note that the estimated values of critical points in this region agree very well with other DMRG data [17]. We furthermore note that the SF-MI transition points are estimated via the Tomonaga-Luttinger exponent K_b as explained in Ref. [18].

As stressed above the various excitation gaps behave differently in the HI phase, in particular at the quantum phase transition points [4, 5]. Figure 1(c) indicates that extrapolated DMRG data of the single-particle gap Δ_c is finite in all insulating phases and closes at the MI-HI transition. By contrast the neutral gap Δ_n closes at both the MI-HI and HI-DW transitions.

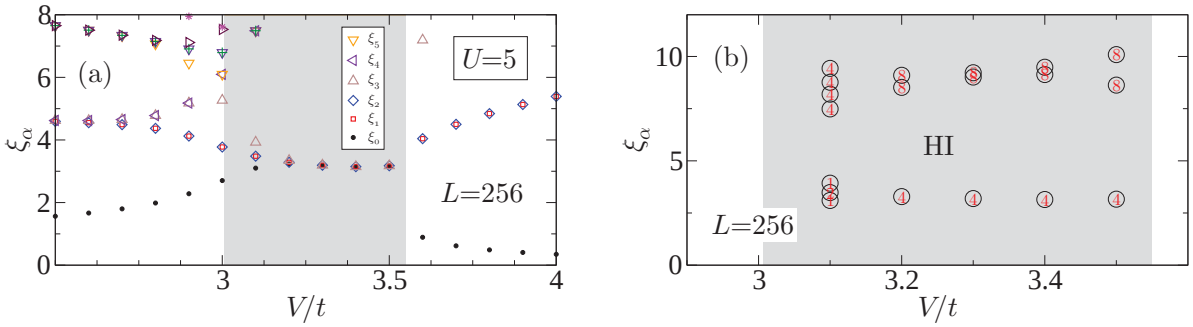

Figure 2. Entanglement spectrum ξ_α of the EBHM with $U/t = 5$, as obtained by DMRG for a system with $L = 256$. The shaded regions mark the HI phase, which shows (at least) a fourfold degeneracy of the lowest [panel (a)] and higher entanglement levels [panel (b)]. The numbers in panel (b) give the degree of degeneracy.

Let us now discuss the topological properties in terms of the entanglement spectra ξ_α within the intermediate-coupling regime ($U/t = 5$). Dividing the system in two halves, using the finite-system DMRG algorithm with PBC, one of the subblock with $L/2$ sites possesses two edges [6, 11]. This has to be contrasted with the infinite-time evolving block-decimation algorithm [3], where only a single edge emerges for the semi-infinite chain. Here we expect a fourfold degeneracy of the lowest entanglement level of the HI phase, just as for the nontrivial topological Haldane phase in the spin-1 XXZ chain. Figure 2(a) brings out this characteristic fourfold degeneracy of the lowest entanglement levels of the EBHM with $n_b = 3$—deep in the HI phase. Since the HI phase is protected by the lattice inversion symmetry in a nontrivial way, not only the lowest but the entire spectrum shows a $4j$-fold degeneracy with $j = 1, 2, \ldots$, as can be seen from Fig. 2(b). In contrast the lowest entanglement levels of the MI and DW phases are apparently non-degenerate. Close to the MI-HI transition larger system sizes $L > 256$ are needed to reproduce the fourfold degeneracy; because of $c = 1$ the gap closes exponentially.

We finally want to take a look at the dynamical properties of EBHM within the range of the topological HI phase, and therefore consider again the intermediate-coupling regime, $U/t = 5$. It is well-known that in the Mott insulator phase a gap opens at the momentum $k = 0$ and the spectral weight becomes concentrated in the region $k > \pi/2$ for $\omega \simeq U$ [15, 16]. Increasing V the MI-HI transition occurs, whereupon the gap at $k = 0$ closes according to Fig. 1(c). At the same time the spectral weight will be concentrated at $k > 3\pi/4$ for $\omega \ll U$, as indicated by Fig. 3(a) for $V \simeq 3.01$. Deep inside the HI phase [see panel (b) for $V/t = 3.3$] the gap at $k = 0$ opens again and the dispersion of the maximum in $S(k, \omega)$ acquires a sine-shape as for the spin-1 XXZ chain [6]. Then the interesting question is whether the gap in $S(k, \omega)$ closes again at the HI-DW transition point if V is increases further. The answer is yes, but now the gap closes at momentum $k = \pi$, reflecting the lattice-period doubling within the DW phase. Accordingly, $S(k, \omega)$ follows the behavior of the neutral gap Δ_n shown in Fig. 1(c).

4. Summary

To conclude, we have analyzed the non-trivial topological Haldane insulator phase—showing up in the intermediate-coupling regime of the one-dimensional Bose-Hubbard model with long-range repulsive particle interaction—from an entanglement point of view. Performing large-scale density matrix renormalization group calculations for finite systems with periodic boundary conditions, the MI-HI and HI-DW quantum phase transition lines can be determined from the central charge c^* via the von Neumann entropy. Thereby our unbiased numerical (lattice model) results confirm the corresponding field theoretical (continuum model) predictions $c = 1$ and $1/2$.

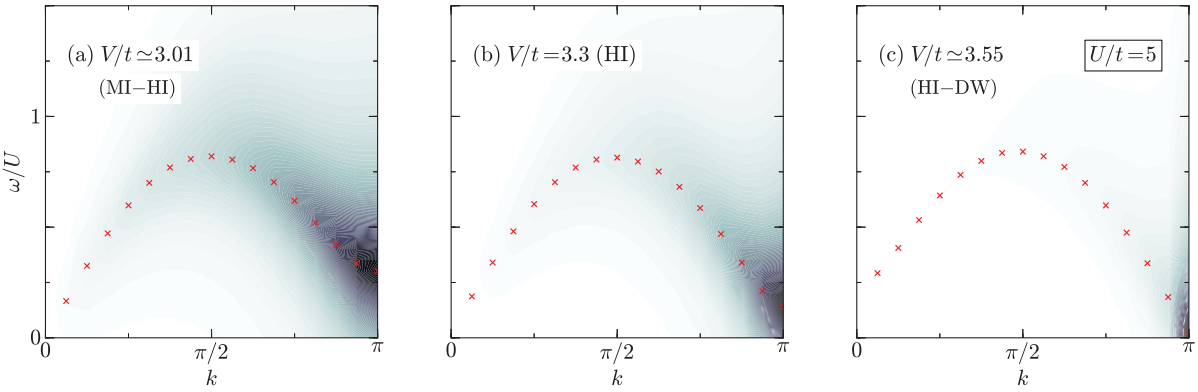

Figure 3. Intensity plots of the dynamical charge structure factor $S(k, \omega)$ at the MI-HI transition point (a), in the HI phase (b), and at the HI-DW transition point (c). Data were obtained applying the DDMRG technique to the 1D EBHM with $L = 32$, using a broadening $\eta = t$. Crosses (circles) give the maximum value of $S(k, \omega)$ at fixed momenta $k = 2\pi j/L$ where $j = 1, \ldots, L/2$.

Furthermore, a characteristic fourfold degeneracy of the lowest entanglement levels in the HI phase is found, which signals the SPT state for the interacting boson model in exactly the same way as for the quantum spin-1 XXZ chain. Finally we studied the dynamical properties of the topological HI phase. Here the dynamical density structure factor is reflective of the behavior of the neutral gap: the dispersion of the maximum in $S(k, \omega)$ is gapless at both the MI-HI and HI-DW transition lines. Notably the momentum where the gap closes differs: for the MI-HI (HI-DW) phase transition the gap vanishes at $k = 0$ ($k = \pi$).

Acknowledgments

The authors would like to thank Y. Fuji and F. Pollmann for valuable discussions. This work was supported by Deutsche Forschungsgemeinschaft through SFB 652, Project B5. The computations were performed at the Regional Computing Center Erlangen.

References

[1] Haldane F D M 1983 *Phys. Rev. Lett.* **50**(15) 1153–1156
[2] Gu Z C and Wen X G 2009 *Phys. Rev. B* **80**(15) 155131
[3] Pollmann F, Berg E, Turner A M and Oshikawa M 2012 *Phys. Rev. B* **85**(7) 075125
[4] Dalla Torre E G, Berg E and Altman E 2006 *Phys. Rev. Lett.* **97** 260401
[5] Berg E, Dalla Torre E, Giamarchi T and Altman E 2008 *Phys. Rev. B* **77** 245119
[6] Ejima S, Lange F and Fehske H 2014 *Phys. Rev. Lett.* **113** 020401
[7] White S R 1992 *Phys. Rev. Lett.* **69** 2863
[8] Jeckelmann E 2002 *Phys. Rev. B* **66** 045114
[9] Jeckelmann E and Fehske H 2007 *Rivista del Nuovo Cimento* **30** 259
[10] Li H and Haldane F D M 2008 *Phys. Rev. Lett.* **101**(1) 010504
[11] Ejima S and Fehske H 2015 *Phys. Rev. B* **91** 045121
[12] Nishimoto S 2011 *Phys. Rev. B* **84** 195108
[13] Clément D, Fabbri N, Fallani L, Fort C and Inguscio M 2009 *Phys. Rev. Lett.* **102** 155301
[14] Ernst P T, Götze S, Krauser J S, Pyka K, Lühmann D S, Pfannkuche D and Sengstock K 2009 *Nature Physics* **6** 56
[15] Ejima S, Fehske H, Gebhard F, zu Münster K, Knap M, Arrigoni E and von der Linden W 2012 *Phys. Rev. A* **85**(5) 053644
[16] Ejima S, Fehske H and Gebhard F 2012 *J. Phys. Conf. Ser.* **391** 012143
[17] Rossini D and Fazio R 2012 *New J. Phys.* **14** 065012
[18] Ejima S, Fehske H and Gebhard F 2011 *Europhys. Lett.* **93** 30002